Effect of optical purity on the critical heat capacity at the smectic-*A*–(chiral)-smectic-*C* transition in an antiferroelectric liquid crystal

Kenji Ema, Masashi Kanai, and Haruhiko Yao
Department of Physics, Faculty of Science, Tokyo Institute of Technology, 2-12-1 Oh-okayama, Meguro, Tokyo 152-8551, Japan

Yoichi Takanishi and Hideo Takezoe
Department of Organic and Polymeric Materials, Faculty of Engineering, Tokyo Institute of Technology, 2-12-1 Oh-okayama, Meguro, Tokyo 152-8552, Japan

(Received 14 May 1999; revised manuscript received 19 October 1999)

High resolution ac calorimetric measurements have been carried out near the smectic-*A*–chiral-smectic-*C* phase transition in the antiferroelectric liquid crystal 4-(1-methylheptyloxycarbonyl)phenyl 4′-octyloxybiphenyl-4-carboxylate (MHPOBC). Data on samples with different optical purities have been analyzed in detail using a renormalization-group expression with corrections-to-scaling terms. The chiral-smectic-C_α–chiral-smectic-*C* phase transition is first order, while the smectic-*A*–chiral-smectic-C_α phase transition is second order. A direct smectic-*A*–chiral-smectic-*C* phase transition, which occurs in near-racemic mixtures, was found to be quasitricritical and weakly first order. This implies that the smectic-*A*–smectic-*C* transition in the racemate locates at a special point where four critical lines intersect.

PACS number(s): 64.70.Md, 61.30.−v, 64.60.Fr, 65.20.+w

I. INTRODUCTION

It has been recently found that the heat capacity of 4-(1-methylheptyloxycarbonyl)phenyl 4′-octyloxybiphenyl-4-carboxylate (MHPOBC) near the smectic A(Sm-A)–chiral-smectic C_α(Sm-C_α*) transition shows critical fluctuation effect which can be described by the three-dimensional (3D) XY model in the immediate vicinity of the transition temperature T_c [1]. While this result is in agreement with the prediction of theory [2], it is quite unusual in the sense that almost all experimental studies of Sm-A–Sm-C or Sm-A–Sm-C* transitions reveal mean-field behavior that is well described by the extended Landau theory [3–7].

Furthermore, it has also been found that the heat capacity of a racemic mixture of MHPOBC exhibits a Gaussian tricritical behavior at the Sm-A–Sm-C transition [8]. This result is apparently compatible with the recent experimental observation that the critical heat capacity in MHPOBC and related substances exhibits crossover from 3D XY to Gaussian tricritical behavior [9]. Thus it is of particular interest to know how nearly-tricritical behavior changes into tricritical behavior as the optical purity is decreased.

Another feature of interest in MHPOBC is the significant effect of the optical purity on the phase sequence. The phase sequences of optically pure MHPOBC and a racemic mixture of MHPOBC are shown in Fig. 1 together with the molecular structure [10,11]. Here Sm-A is a paraelectric phase, Sm-C* is a ferroelectric phase, Sm-C_α* and Sm-C_A* are antiferroelectric phases, Sm-C_γ* is a ferrielectric phase, and I stands for the isotropic phase. It was found that the stability range of the Sm-C_α* phase and Sm-C_γ* phase diminishes in optically impure systems [11].

In this paper we report the results of ac calorimetric measurements on R-S mixtures of MHPOBC for various mixture ratios. The Sm-C_α*–Sm-C* phase transition is first order, while the Sm-A–Sm-C_α* phase transition is second-order. The direct Sm-A–Sm-C* phase transition, which occurs in near-racemic mixtures, was found to be quasitricritical and weakly first order. This implies that the transition in the racemate locates at a special point where four critical lines intersect.

II. RESULTS

The heat capacity was measured using an ac calorimeter described elsewhere [12]. Samples with several mixture ratios of the two enantiomers were prepared by mixing S-MHPOBC and racemate MHPOBC. The mixture ratios will be referred to by citing the mole percent X of the S enantiomer in the mixture. Hermetically sealed gold cells which contained about 30 mg of liquid crystal sample were used. Temperature scan rate was about 0.03 K/h in the transition region. Very slow drift rates in the Sm-A–Sm-C_α* (or C*) transition temperature, typically −2 to −4 mK/day, in-

MHPOBC $C_8H_{17}O$-⟨⟩-⟨⟩-COO-⟨⟩-$COOC^*H(CH_3)C_6H_{13}$

Phase sequence of optically pure MHPOBC

$$\mathrm{Sm}-C_A^* \underset{392.3\mathrm{K}}{\longleftrightarrow} \mathrm{Sm}-C_\gamma^* \underset{393.0\mathrm{K}}{\longleftrightarrow} \mathrm{Sm}-C^* \underset{395.0\mathrm{K}}{\longleftrightarrow} \mathrm{Sm}-C_\alpha^* \underset{396.3\mathrm{K}}{\longleftrightarrow} \mathrm{Sm}-A \underset{421\mathrm{K}}{\longleftrightarrow} I.$$

Phase sequence of racemate MHPOBC

$$\mathrm{Sm}-C_A \underset{387.1\mathrm{K}}{\longleftrightarrow} \mathrm{Sm}-C \underset{394.8\mathrm{K}}{\longleftrightarrow} \mathrm{Sm}-A \underset{421\mathrm{K}}{\longleftrightarrow} I.$$

FIG. 1. Molecular structure of MHPOBC, and phase sequences of optically pure MHPOBC and a racemic mixture of MHPOBC. The transition temperatures are based on the present measurement on heating.

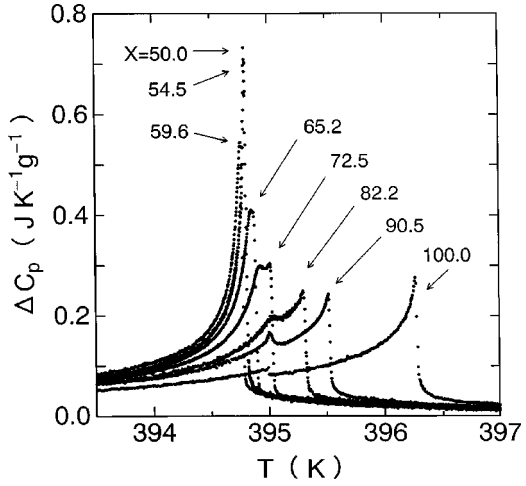

FIG. 2. Temperature dependence of the excess heat capacity ΔC_p for MHPOBC for various values of X, the mole percent of S enantiomer. Data for $X=100$ are from [1], and those for $X=50$ are from [8]. Data for $X=50$ and $X=54.5$ overlay so closely that they look like one set of points in this scale.

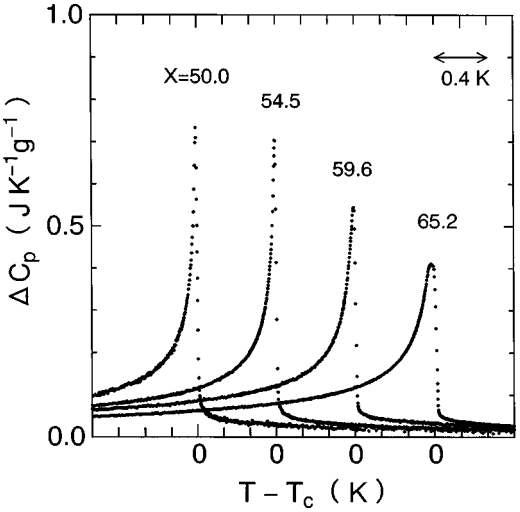

FIG. 3. Temperature dependence of the excess heat capacity ΔC_p for the Sm-A–Sm-C^* transition in MHPOBC with $X=50$, 54.5, 59.6, and 65.2. To avoid overlap of the data, the temperature scale has been shifted for each data set.

dicate the stability and high quality of the sample.

The C_p values were determined from the following expression:

$$C_p=(C_p^{\text{obs}}-C_p^{\text{empty}})/m. \tag{1}$$

Here C_p^{obs} and C_p^{empty} are the heat capacity of the filled cell and the empty cell, respectively, and m is the mass of the liquid-crystal sample in grams. The background heat capacity C_p(background) was determined as a quadratic function of the temperature which joins the observed heat capacity data smoothly at temperatures away from the transition on both sides. The excess heat capacity ΔC_p was obtained as

$$\Delta C_p=C_p-C_p(\text{background}). \tag{2}$$

The ΔC_p data for all values of X studied in the present work are shown in Fig. 2 [13]. The results for the optically pure sample ($X=100$) and the racemic mixture ($X=50$) are also included. The data for the racemic and near-racemic mixtures, $X=65.2$, 59.6, 54.4, and 50, are shown as a function of $\Delta T=T-T_c$ in Fig. 3.

A. Results for high optical-purity samples

For relatively high optical-purity samples, $X=100$, 90.5, 82.2, and 72.5, the data show two C_p peaks in the temperature range displayed in Fig. 2, corresponding to the Sm-A–Sm-C_α^*–Sm-C^* phase sequence. The Sm-A–Sm-C_α^* transition is located at around 396.3, 395.5, 395.3, and 395.1 K, respectively, where a sharp ΔC_p peak is seen. On the other hand, only a small C_p cusp is seen at the Sm-C_α^*–Sm-C^* transitions, located at around 395.0, 395.0, 395.1, and 394.9 K. The temperature width of the Sm-C_α^* phase is 1.3, 0.50, 0.26, and 0.10 K, respectively.

In ac calorimetry, the existence of a two-phase coexistence region at a first-order transition is often detected as an abrupt change in the phase lag of the ac temperature response (see Fig. 5 of Ref. [14]). Figure 4 shows the temperature dependence of the phase lag ϕ near the transitions of the sample $X=90.5$. A distinct peak is seen at the Sm-C_α^*–Sm-C^* transition, indicating that this transition is first order. On the other hand, only a small steplike variation is seen at the Sm-A–Sm-C_α^* transition. A possibility that this small step could correspond to a very weak first order transition is excluded as follows. The phase lag ϕ is given to the first order as

$$\phi=\frac{1}{\omega\tau_{\text{e}}}-a\omega\tau_{\text{i}}, \tag{3}$$

where ω is the angular frequency of the ac heating, τ_{e} and τ_{i} are so-called external and internal relaxation times [15,16], and a is a model-dependent constant [17]. Equation (3) shows that ϕ can exhibit an anomaly due to the temperature dependence of the sample heat capacity C_p through τ_{e} and τ_{i} [16] even in the absence of two-phase coexistence. In most cases the variation of C_p is relatively small in comparison with the total heat capacity and therefore Eq. (3) implies a linear relationship between ϕ and C_p. In Fig. 5 data near the

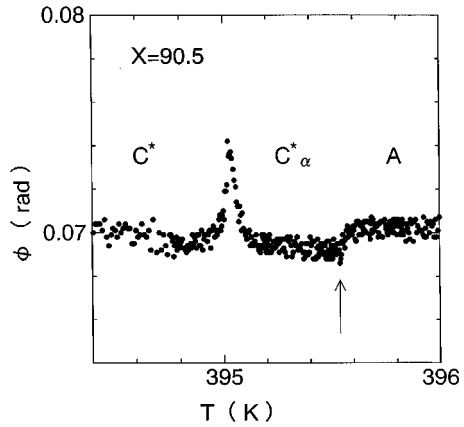

FIG. 4. Temperature dependence of the phase lag ϕ for MHPOBC with $X=90.5$. Arrow shows the Sm-A–Sm-C_α^* transition temperature.

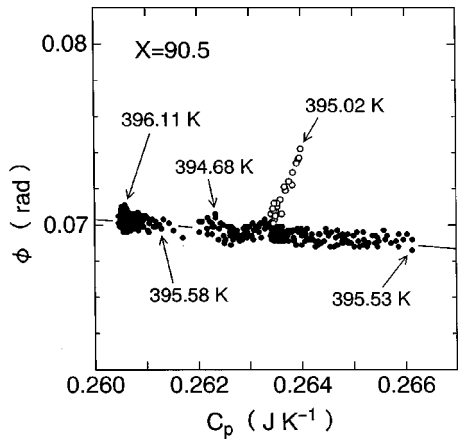

FIG. 5. Plot of data of the phase lag ϕ against C_p for MHPOBC with $X=90.5$. Solid line is a guide to the eye. In this plot, C_p is the total heat capacity of the sample cell including the liquid crystal sample and the gold cell.

transitions are plotted on a ϕ-C_p plane. It is obvious that a step of ϕ seen in Fig. 4 at 395.53–395.58 K is consistent with a linear relationship between ϕ and C_p as indicated by the slanting line shown in Fig. 5, while the odd behavior of ϕ around 395.02 K, shown as open circles, corresponds to the two phase coexistence region due to the Sm-C_α*–Sm-C* transition. From these considerations, the Sm-A–Sm-C_α* transition is expected to be of the second order. The same behavior was observed for $X=82.2$ and 72.5 samples.

B. Results for near-racemic samples

It is seen in Fig. 3 that racemic and near-racemic mixtures, $X=65.2$, 59.6, 54.5, and 50.0, undergo a direct Sm-A–Sm-C* phase transition. It is seen that the magnitude and the shape of the anomaly in each case is similar to that in the racemic mixture except in the immediate vicinity of the transition temperature. For $X=54.5$ and 59.6, ΔC_p is clearly a single peak, indicating the absence of the Sm-C_α* phase. The results for $X=65.2$ seem marginal: ΔC_p can probably be viewed as a single peak, but it may also be possible to regard it as a closely spaced combination of a high-temperature sharp peak and a low-temperature broad peak.

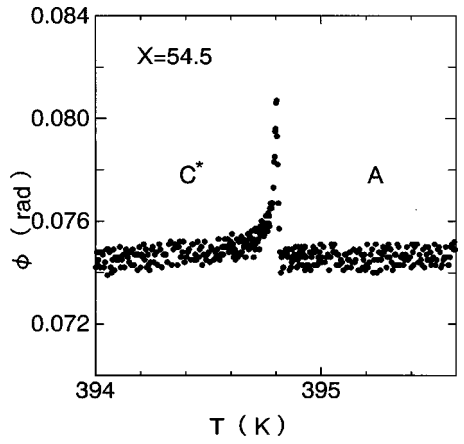

FIG. 6. Temperature dependence of the phase lag ϕ for MHPOBC with $X = 54.5$.

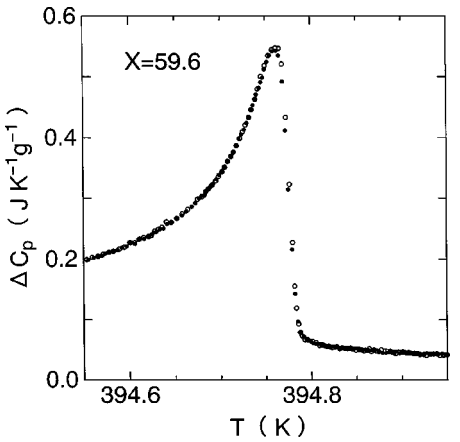

FIG. 7. A comparison of heating (filled circles) and cooling (open circles) data near the Sm-A–Sm-C* transition temperature for the $X=59.6$ sample.

Figure 6 shows the temperature dependence of the phase lag ϕ near the transition for the sample $X=54.5$. The data show a distinct peak at the Sm-A–Sm-C* transition, indicating that this transition is first order. Similar anomalies in ϕ were also observed in $X=59.6$ and $X=65.2$ samples. Assuming that these anomalies in the phase correspond to coexisting phase regions, their widths are 16, 38, and 98 mK for $X=54.5$, 59.6, and 65.2 samples, respectively.

Figure 7 shows a comparison of typical heating and cooling data near the heat capacity peak obtained for the $X=59.6$ sample. It is seen that the heating and cooling data agree quite well. This shows that the first-order nature of the present transition is very weak.

III. ANALYSIS

The ΔC_p data around the Sm-A–Sm-C_α* transition have been analyzed with the following renormalization-group expression including corrections-to-scaling terms [18,19]:

$$\Delta C_p=\frac{A^{\pm}}{\alpha}|t|^{-\alpha}(1+D_1^{\pm}|t|^{\theta}+D_2^{\pm}|t|)+B_c, \qquad (4)$$

where $t\equiv(T-T_c)/T_c$ and the superscripts $\pm$ denote above and below T_c. We note that the use of this expression for the analysis of the present data in near-racemic samples showing first-order Sm-A–Sm-C* transitions can be justified as a starting trial function, because the first-order nature of the transition is very weak as pointed out above.

The exponent α was usually adjusted freely in the least-squares fitting procedure. The correction-to-scaling exponent θ is actually dependent on the universality class, but has a theoretically predicted value quite close to 0.5 [18]. Therefore, its value is fixed at 0.5 unless otherwise stated. Fits were made for the data over three ranges, $|t|_{\max}=0.001$, 0.003, and 0.01, where $|t|_{\max}$ is the maximum value of $|t|$ used in the fit. The value of T_c was chosen as follows. Although we do not know the value of T_c *a priori*, it is inconsistent to use different T_c's for different data ranges. Therefore we fixed T_c to the value determined in the narrowest data range for each set of fits using the same fitting expression. There is usually a narrow region very close to T_c

TABLE I. Least-squares values of the adjustable parameters for fitting ΔC_p with Eq. (4) for $X=90.5$. The minimum reduced temperatures for $T>T_c$ and $T<T_c$ are typically $t^+_{\min}=4\times10^{-5}$ and $|t^-_{\min}|=3\times10^{-5}$. The number of fitted data points N was 214, 357, and 836 for $|t|_{\max}=0.001$, 0.003, and 0.01, respectively. The number of degree of freedom ν is given as $\nu=N-p$, where p is the number of free parameters. Quantities in brackets were held fixed at the given values. The units are J K^{-1} g^{-1} for A^+ and B_c, and K for T_c.

$\lvert t\rvert_{\max}$	T_c	α	θ	10^3A^+	A^-/A^+	D_1^+	D_1^-	D_2^+	D_2^-	B_c	χ^2_ν
0.001	395.530	0.035	[0.5]	9.93	1.482	1.04	−2.94	[0]	[0]	−0.341	1.00
0.003	[395.530]	0.050	[0.5]	6.39	1.921	−0.31	−4.99	[0]	[0]	−0.147	1.50
0.01	[395.530]	0.119	[0.5]	3.01	3.49	−4.77	−6.80	[0]	[0]	−0.017	8.12
0.01	[395.530]	0.009	[0.5]	8.95	1.182	−0.03	−2.42	−0.28	11.24	−1.025	1.42
0.001	395.523	[−0.0066]	[0.524]	19.15	0.933	−0.33	0.71	[0]	[0]	2.780	1.11
0.003	[395.523]	[−0.0066]	[0.524]	17.26	0.929	−0.19	0.80	[0]	[0]	2.517	3.07
0.01	[395.523]	[−0.0066]	[0.524]	23.00	0.953	−0.16	0.34	[0]	[0]	3.345	26.4
0.01	[395.523]	[−0.0066]	[0.524]	12.27	0.893	−0.09	2.16	0.55	−9.71	1.805	1.47

where data are artificially rounded due to impurities or instrumental effects, and the data inside this region have been excluded in the fitting.

A. High optical-purity samples

Table I shows the parameter values obtained for the $X=90.5$ sample. To avoid the C_p anomaly due to the Sm-C_α*–Sm-C* transition, data in the range 394.1 K$<T<$395.0 K have been excluded. It is assumed that data $T<394.1$ K in the Sm-C* phase are same as what would be expected for the Sm-C_α* phase if it existed [9]. When only a first-order correction term is included, the results show the following: (A) The α value is close to the 3D XY value of −0.0066 [18] for narrow data ranges, while it increases significantly as data range becomes wider. (B) XY fits where the exponents are fixed at 3D XY values give reasonably good fits except for the violation of the theoretical expectation of $D_1^+\sim D_1^-$ [20,21]. These trends are similar to those seen in the optically pure sample $X=100$ [1,9]. Inclusion of second-order correction terms improves the quality of the fits substantially. The α value when freely adjustable is $\alpha=0.009$, which is close to the 3D XY theoretical value. However, $D_1^+\neq D_1^-$ persists in the XY fit. Although the ratio D_2^-/D_2^+ is not universal [19], the present value for the XY fit $D_2^-/D_2^+=-17.6$ seems rather large in comparison with D_2^-/D_2^+ being within ±2 obtained for the nematic–Sm-A transitions showing a typical 3D XY behavior [19,22]. Further, allowing nonzero $D_2^\pm$ moves the critical amplitude ratio away from the 3D XY theoretical value 0.971. These facts make us to speculate that the improvement of the fit with inclusion of second-order terms could be rather artificial.

Table II shows the parameter values obtained for $X=82.2$ sample. Data in the range 394.8 K$<T<$395.2 K, associated with the Sm-C_α*–Sm-C* transition, have been excluded from the fits. The results are similar to those for the $X=90.5$ sample. The parameter values for $|t|_{\max}=0.001$ are not shown because the effect from the subpeak gap is too large.

B. Near racemic samples

Table III shows the values of adjustable parameters obtained in fits to the data for the $X=54.5$ sample with Eq. (4). It is seen that the fits yield α values close to the tricritical value 0.5. It is also noticed that the values of $D_1^\pm$ are anomalously large, and are unstable against data-range shrinking. Such a feature is qualitatively similar to that seen in the racemate [8]. However, the physical significance of these fits seems doubtful since A^+ is anomalously small and D_1^+ is anomalously large. In our opinion, these fits are artificial due not only to the almost tricritical nature but also to the first-order nature of the transition. If $\alpha>0.5$ and $\theta=0.5$, the correction term $A^\pm D_1^\pm|t|^{\theta-\alpha}$ will diverge at T_c rather than go to zero as it should.

We next fitted the data with the following expression:

TABLE II. Least-squares values of the adjustable parameters for fitting ΔC_p with Eq. (4) for $X=82.2$. The minimum reduced temperatures for $T>T_c$ and $T<T_c$ are typically $t^+_{\min}=5\times10^{-5}$ and $|t^-_{\min}|=10\times10^{-5}$. The number of fitted data points N was 331 and 779 for $|t|_{\max}=0.003$ and 0.01, respectively. The number of degree of freedom ν is given as $\nu=N-p$, where p is the number of free parameters. Quantities in brackets were held fixed at the given values. The units are J K^{-1} g^{-1} for A^+ and B_c, and K for T_c.

$\lvert t\rvert_{\max}$	T_c	α	θ	10^3A^+	A^-/A^+	D_1^+	D_1^-	D_2^+	D_2^-	B_c	χ^2_ν
0.003	395.340	0.043	[0.5]	3.22	3.118	−2.90	−9.30	[0]	[0]	−0.064	1.49
0.01	[395.340]	0.222	[0.5]	0.457	17.10	−71.7	−11.0	[0]	[0]	0.040	3.65
0.01	[395.340]	0.024	[0.5]	3.56	2.359	−2.15	−11.1	7.2	56.3	−0.137	1.63
0.003	395.320	[−0.0066]	[0.524]	11.44	0.869	−0.08	2.17	[0]	[0]	1.684	1.70
0.01	[395.320]	[−0.0066]	[0.524]	27.73	0.957	−0.20	28.6	[0]	[0]	4.017	16.7
0.01	[395.320]	[−0.0066]	[0.524]	10.26	0.843	−0.06	3.90	0.43	−19.3	1.511	1.71

TABLE III. Least-squares values of the adjustable parameters for fitting ΔC_p with Eq. (4) for $X=54.5$. The minimum reduced temperatures for $T>T_c$ and $T<T_c$ are $t^+_{\min}=1\times10^{-5}$ and $|t^-_{\min}|=6\times10^{-5}$. The number of fitted data points N was 208, 499, and 919 for $|t|_{\max}=0.001$, 0.003, and 0.01, respectively. The number of degree of freedom ν is given as $\nu=N-p$, where p is the number of free parameters. Quantities in brackets were held fixed at the given values. The units are J K^{-1} g^{-1} for A^+ and B_c, K for T_c.

$\|t\|_{\max}$	T_c	α	10^4A^+	A^-/A^+	D_1^+	D_1^-	D_2^+	D_2^-	B_c	χ^2_ν
0.001	394.816	0.571	0.245	51.4	1668	33.1	[0]	[0]	−0.087	1.01
0.003	[394.816]	0.562	0.205	65.9	2691	40.1	[0]	[0]	−0.119	1.03
0.01	[394.816]	0.560	0.118	115.7	5394	45.8	[0]	[0]	−0.139	1.13
0.01	[394.816]	0.568	0.306	42.4	1179	27.7	−1544	−40.6	−0.067	0.94

$$\Delta C_p=\frac{A^\pm}{\alpha}|t|^{-\alpha}(1+D_2^\pm|t|)+B^\pm, \tag{5}$$

where $\Delta B\equiv B^+-B^-\neq0$. The use of this form has been motivated partly because the first correction term behaves like a constant term when $\alpha\cong0.5$ and $\theta\cong0.5$ If α and θ were exactly 1/2, the correction term would become $A^\pm D_1^\pm$, giving $B^\pm=B_c+A^\pm D_1^\pm$ which can differ above and below T_c. Note also that the scaling requirement $B^+=B^-$ need not be fulfilled for first-order transitions. The first four lines in Table IV show the results of fits with Eq. (5). Because higher-order correction terms are expected to have significant influence only away from T_c, results with nonzero $D_2^\pm$ are shown only for the widest data range, $|t|_{\max}=0.01$. The α values are still close to 0.5 in all these fits.

At first-order transitions, the temperature where ΔC_p diverges will be different when the transition is approached from the higher or lower temperature side. This can be taken into account by replacing the reduced temperature t by

$$t^\pm\equiv\frac{T-T_c^\pm}{T_c^\pm}, \tag{6}$$

where superscripts $\pm$ denote above and below T_c. It is expected that T_c^+ is lower than T_c^-, thus

$$\Delta T_c\equiv T_c^- - T_c^+ \tag{7}$$

should be positive. The middle four lines in Table IV show the results of allowing a nonzero ΔT_c. Fits were also tried fixing α at the tricritical value 0.5, while ΔT_c was allowed to have nonzero values. The results are shown in the last four lines.

Similar fits were tried for $X=59.6$ and $X=65.2$ samples. It was found that fitting the data with Eq. (4) in these cases resulted in unphysical results with negative A^-/A^+, and therefore such fits are not shown here. Tables V and VI show the results of the fits with Eq. (5) to $X=59.6$ and $X=65.2$, respectively. It is seen from Tables IV–VI that the α show almost tricritical values in all three cases. The fits obtained by fixing α at 0.5 are as good as those with α freely adjusted. It is also to be noted that the value of ΔT_c, when allowed to be nonzero, increases in the order of $X=54.5$, 59.6, and 65.2. This indicates that the first-order nature of the transition becomes more significant as X increases.

TABLE IV. Least-squares values of the adjustable parameters for fitting ΔC_p with Eq. (5) for $X=54.5$. Here $\Delta B=B^+-B^-$, and $\Delta T_c=T_c^- - T_c^+$. The minimum reduced temperatures for $T>T_c$ and $T<T_c$ are typically $t^+_{\min}=3\times10^{-5}$ and $|t^-_{\min}|=7\times10^{-5}$. The number of fitted data points N was 208, 499, and 919 for $|t|_{\max}=0.001$, 0.003, and 0.01, respectively. The number of degree of freedom ν is given as $\nu=N-p$, where p is the number of free parameters. Quantities in brackets were held fixed at the given values. The units are J K^{-1} g^{-1} for A^+, B^+, and ΔB, and K for T_c^+ and ΔT_c.

$\|t\|_{\max}$	T_c^+	ΔT_c	α	10^4A^+	A^-/A^+	D_2^+	D_2^-	B^+	ΔB	χ^2_ν
0.001	394.809	[0]	0.436	3.64	10.02	[0]	[0]	0.018	0.044	1.26
0.003	[394.809]	[0]	0.442	3.91	8.87	[0]	[0]	0.014	0.035	2.70
0.01	[394.809]	[0]	0.436	4.89	7.38	[0]	[0]	0.007	0.030	6.07
0.01	[394.809]	[0]	0.452	2.93	10.91	−402	−4.5	0.024	0.040	1.09
0.001	394.806	0.005	0.466	3.03	9.71	[0]	[0]	0.018	0.032	1.23
0.003	[394.806]	[0.005]	0.462	3.51	8.65	[0]	[0]	0.014	0.029	2.09
0.01	[394.806]	[0.005]	0.450	4.59	7.23	[0]	[0]	0.007	0.027	5.73
0.01	[394.806]	[0.005]	0.477	2.50	10.69	−452	−14.2	0.026	0.030	1.05
0.001	394.805	0.008	[0.5]	2.32	9.89	[0]	[0]	0.020	0.020	1.26
0.003	[394.805]	[0.008]	[0.5]	2.63	8.83	[0]	[0]	0.016	0.018	2.51
0.01	[394.805]	[0.008]	[0.5]	3.16	7.43	[0]	[0]	0.010	0.015	7.86
0.01	[394.805]	[0.008]	[0.5]	2.08	10.95	−540	−24.6	0.027	0.023	1.04

TABLE V. Least-squares values of the adjustable parameters for fitting ΔC_p with Eq. (5) for $X=59.6$. Here $\Delta B=B^+-B^-$, and $\Delta T_c=T_c^- - T_c^+$. The minimum reduced temperatures for $T>T_c$ and $T<T_c$ are typically $t_{\min}^+=5\times10^{-5}$ and $|t_{\min}^-|=11\times10^{-5}$. The number of fitted data points N was 173, 460, and 901 for $|t|_{\max}=0.001,\ 0.003$, and 0.01, respectively. The number of degree of freedom ν is given as $\nu=N-p$, where p is the number of free parameters. Quantities in brackets were held fixed at the given values. The units are J K^{-1} g^{-1} for A^+, B^+, and ΔB, and K for T_c^+ and ΔT_c.

$\lvert t\rvert_{\max}$	T_c^+	ΔT_c	α	10^4A^+	A^-/A^+	D_2^+	D_2^-	B^+	ΔB	χ_ν^2
0.001	394.770	[0]	0.413	3.42	12.99	[0]	[0]	0.021	0.062	1.11
0.003	[394.770]	[0]	0.443	3.47	9.96	[0]	[0]	0.015	0.034	3.71
0.01	[394.770]	[0]	0.423	5.25	7.60	[0]	[0]	0.006	0.033	7.16
0.01	[394.770]	[0]	0.464	1.975	14.79	−793	−15.2	0.028	0.088	1.45
0.001	394.758	0.023	0.541	1.468	12.43	[0]	[0]	0.024	0.017	1.04
0.003	[394.758]	[0.023]	0.529	2.09	9.56	[0]	[0]	0.017	0.013	3.03
0.01	[394.758]	[0.023]	0.479	3.94	7.33	[0]	[0]	0.007	0.021	6.85
0.01	[394.758]	[0.023]	0.583	0.807	15.75	−1700	−99.0	0.039	0.000	1.33
0.001	394.761	0.016	[0.5]	1.955	12.33	[0]	[0]	0.020	0.028	1.04
0.003	[394.761]	[0.016]	[0.5]	2.52	9.51	[0]	[0]	0.013	0.019	3.03
0.01	[394.761]	[0.016]	[0.5]	3.26	7.46	[0]	[0]	0.005	0.014	7.70
0.01	[394.761]	[0.016]	[0.5]	1.673	14.13	−868	−19.9	0.029	0.030	1.43

IV. DISCUSSION

Figure 8 shows a partial temperature-concentration phase diagram obtained from the present work. The solid line shows first-order transitions, and the dashed line shows a second-order transition. This result agrees with the phase diagram reported earlier based on DSC (differential scanning calorimetry) [11] except for some of details. One of the differences between the present results and the former ones is that the Sm-C_α* phase does not disppear until relatively low optical purity. Although the Sm-C_α* phase was not detected for $X=80$ in the DSC study, it is clearly visible here at $X\sim72$. This disagreement is not surprising since DSC measurements are usually less sensitive and are carried out at much faster scan rates [23].

The present data indicate that the Sm-A–Sm-C_α* transition is second-order at least for $X\geqslant82.2$. The critical nature of the Sm-A–Sm-C_α* transition is almost unaffected by the presence of the Sm-C_α*–Sm-C* transition. In particular, there is no indication that the Sm-A–Sm-C_α* transition approaches a tricritical point as X decreases, at least down to $X\sim72$. This leads us to exclude a scenario in which the second-order Sm-A–Sm-C_α* transition observed for the optically pure MHPOBC changes smoothly into the tricritical behavior seen for the racemate. If the Sm-A–Sm-C_α* transition remains second-order as far as the Sm-C_α* phase exists, the Sm-A–Sm-C_α* transition line ends up with a critical-end point (CEP) because both the Sm-C_α*–Sm-C* and the Sm-A–Sm-C* transitions are believed to be first-order. If this is the case, it seems reasonable that the Sm-C_α*–Sm-C* transition line does not simply merge the

TABLE VI. Least-squares values of the adjustable parameters for fitting ΔC_p with Eq. (5) for $X=65.2$. Here $\Delta B=B^+-B^-$, and $\Delta T_c=T_c^- - T_c^+$. The minimum reduced temperatures for $T>T_c$ and $T<T_c$ are typically $t_{\min}^+=7\times10^{-5}$ and $|t_{\min}^-|=17\times10^{-5}$. The number of fitted data points N was 183, 470, and 911 for $|t|_{\max}=0.001,\ 0.003$, and 0.01, respectively. The number of degree of freedom ν is given as $\nu=N-p$, where p is the number of free parameters. Quantities in brackets were held fixed at the given values. The units are J K^{-1} g^{-1} for A^+, B^+, and ΔB, and K for T_c^+ and ΔT_c.

$\lvert t\rvert_{\max}$	T_c^+	ΔT_c	α	10^4A^+	A^-/A^+	D_2^+	D_2^-	B^+	ΔB	χ_ν^2
0.001	394.879	[0]	0.353	5.36	13.98	[0]	[0]	0.019	0.110	1.52
0.003	[394.879]	[0]	0.434	3.48	11.42	[0]	[0]	0.018	0.047	5.07
0.01	[394.879]	[0]	0.433	4.72	8.39	[0]	[0]	0.010	0.037	14.92
0.01	[394.879]	[0]	0.452	1.992	17.42	−738	−1.7	0.032	0.052	1.78
0.001	394.852	0.054	0.584	1.189	13.47	[0]	[0]	0.025	0.022	1.38
0.003	[394.852]	[0.054]	0.589	1.400	10.95	[0]	[0]	0.021	0.013	3.76
0.01	[394.852]	[0.054]	0.536	2.77	8.04	[0]	[0]	0.011	0.019	13.88
0.01	[394.852]	[0.054]	0.668	0.380	21.31	−3115	−165	0.048	−0.009	1.21
0.001	394.862	0.034	[0.5]	2.05	13.61	[0]	[0]	0.024	0.044	1.39
0.003	[394.862]	[0.034]	[0.5]	2.50	10.91	[0]	[0]	0.019	0.033	4.62
0.01	[394.862]	[0.034]	[0.5]	3.34	8.14	[0]	[0]	0.011	0.024	13.79
0.01	[394.862]	[0.034]	[0.5]	1.625	16.83	−819	−4.2	0.034	0.049	2.07

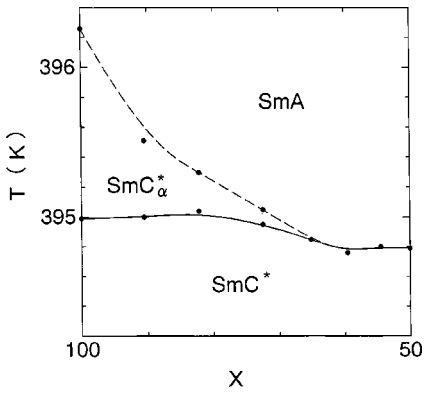

FIG. 8. Partial temperature-concentration phase diagram of MHPOBC obtained in the present work. Solid lines represent first-order transitions, and the dashed line a second-order transition.

Sm-A–Sm-C_α* line tangentialy as drawn in Fig. 8, but makes some finite angle there as usually observed at CEP.

The Sm-A–Sm-C* transition in the absence of the Sm-C_α* phase turned out to be almost tricritical but weakly first order. The main evidence presented here that the Sm-A–Sm-C* transition is first order is the existence of an anomaly in the phase lag ϕ observed in the ac calorimetric measurement. The fact that better fits are obtained by allowing $T_c^+ \neq T_c^-$ also supports the first-order nature of this transition. One could argue that $T_c^+ \neq T_c^-$ might be an artifact caused by a smearing of the transition due to imperfections and/or inhomogeneities in the sample. It should be noticed, however, that smearing of the transition cannot explain the existence of an anomaly in ϕ. On the other hand, regarding the region of anomalous ϕ values as a two-phase coexistence region, this region decreases monotonically and smoothly goes to zero on approaching the racemic point. The difference between T_c^+ and T_c^- determined in the fits described above also behaves in the same way. These facts lead to a reasonable scenario that the weak first-order nature smoothly vanishes and changes into the tricritical behavior observed for the racemic mixture [8].

The phase diagram must be symmetric with respect to the racemate and therefore the transition is first-order on the both sides of $X=50$. Because of this, *four* critical lines meet at the racemic point instead of three lines as in the ordinary tricritical point where the transition changes from second to first order [24,25]. In this sense the racemic point in the present case can be called as a *tetracritical* point according to Nagle and Bonner [26]. Note that this is not contradicted by the fact that α has the tricritical value. As pointed out in Ref. [24], it is impotant to distinguish the order of a critical point from the number of critical lines meeting there, and a tetracritical point which was treated in Ref. [26], and also our present case, is qualitatively the same as a tricritical point. Such a special situation was also found in a ferroelectric crystal [27].

A racemic mixture represents a very special position in a mixture system of two enantiomers since only there does the chirality of system vanish. Therefore, it seems highly improbable that tricriticality would occur at the racemic point just by chance. Quite interestingly, another example is known where a racemic mixture exhibits tricritical behavior at a Sm-A–Sm-C transition: 4-(3-methyl-2-chlorobutanoyloxy) 4′-heptyloxybiphenyl (A7) [28]. Although we do not have any clear theoretical reasoning, it is conceivable that the transition in near racemic mixtures evolves into a tricritical one at $X=50$ due to some symmetrical reason when a certain requirement is satisfied.

The above picture suggests that the transition is driven to first-order by some chiral mechanism, which thus cannot operate in a racemic mixture. The effect of coupling between tilt order and strain in the Sm-A–Sm-C* transition was discussed by Benguigui and Martinoty [29]. They showed that this coupling moves the transition toward a tricritical point. They also showed, however, the order of the transition is not changed by this coupling. Besides, this coupling also exists in a racemate. Therefore, this coupling is probably not responsible in the present case. Another key is that the mechanism is not applicable to the Sm-A–Sm-C_α* transition, since this transition remains second order. Then possible candidates are the macroscopic dipole moment in the direction normal to the tilting plane, and the helix structure. The couplings of these degrees of freedom with strain have not been investigated in detail especially in the presence of a significant fluctuation effect, and therefore we should wait for future developement of theory.

Finally, we add here one more remark. In principle, we cannot rule out the possibility of a very small window of Sm-C_α* region for $X \lesssim 65$ except $X=50$. Under this assumption, the anomaly in the phase ϕ as shown in Fig. 6 is understood to be caused by the first-order Sm-C_α*–Sm-C* transition, and therefore the Sm-A–Sm-C_α* transition need not be first-order. On the other hand, we encounter a new problem to explain the reason why the Sm-C_α* phase persists as far as the chirality exists. Further, now we expect that two first-order transition lines and two critical lines meet at the racemic point, thus the situation seems as complex as before. Because a similar tricritical behavior is seen in a racemic mixture of A7 as mentioned above [28], it is probable that the appearance of the characteristic phase diagram does not need the existence of the Sm-C_α* phase. In any case, detailed studies of the optical impurity effect would be desired on other liquid crystals including A7.

ACKNOWLEDGMENT

We are grateful to C. W. Garland for valuable discussions.

[1] K. Ema, J. Watanabe, A. Takagi, and H. Yao, Phys. Rev. E **52**, 1216 (1995).

[2] P.G. de Gennes, Mol. Cryst. Liq. Cryst. **21**, 49 (1973).

[3] C.C. Huang and J.M. Viner, Phys. Rev. A **25**, 3385 (1982).

[4] C.C. Huang and S. Dumrongrattana, Phys. Rev. A **34**, 5020 (1986).

[5] C.W. Garland, in *Phase Transitions in Liquid Crystals*, Vol. 290 of *NATO Advanced Study Institute, Series B: Physics*, edited by S. Martelucci and A.N. Chester (Plenum, New York, 1992), Chap. 11.

[6] T. Chan, Ch. Bahr, G. Heppke, and C.W. Garland, Liq. Cryst. **13**, 667 (1993).
[7] J. Thoen, Int. J. Mod. Phys. B **9**, 2157 (1995).
[8] K. Ema, A. Takagi, and H. Yao, Phys. Rev. E **53**, R3036 (1996); **55**, 508 (1997).
[9] K. Ema, M. Ogawa, A. Takagi, and H. Yao, Phys. Rev. E **54**, R25 (1996); K. Ema and H. Yao, *ibid.* **57**, 6677 (1998).
[10] A.D.L. Chandani, Y. Ouchi, H. Takezoe, A. Fukuda, K. Terashima, K. Furukawa, and A. Kishi, Jpn. J. Appl. Phys., Part 2 **28**, L1261 (1989); Y. Takanishi, K. Hiraoka, V.K. Agrawal, H. Takezoe, A. Fukuda, and M. Matsushita, Jpn. J. Appl. Phys., Part 1 **30**, 2023 (1991); K. Hiraoka, Y. Takanishi, K. Skarp, H. Takezoe, and A. Fukuda, Jpn. J. Appl. Phys., Part 2 **30**, L1819 (1991).
[11] H. Takezoe, J. Lee, A.D.L. Chandani, E. Gorecka, Y. Ouchi, A. Fukuda, K. Terashima, and K. Furukawa, Ferroelectrics **114**, 187 (1991).
[12] K. Ema and H. Yao, Thermochim. Acta **304/305**, 157 (1997), and references therein.
[13] In the present work, racemate MHPOBC samples of two different origins (called no. 1 and no. 2, hereafter) have been used. Our early measurements [8] were made on sample no. 1, while most of the results shown in the present work have been obtained using racemate sample no. 2. The observed C_p behaviors were identical to each other except that the Sm-A–Sm-C transition temperature of sample no. 2 was 0.30 K higher than that of sample no. 1. Because of this, the temperature scale for the data shown in the present work has been shifted by 0.30 K$\times$ (concentration of racemate) when racemate sample no. 1 was used. This amounts to 0.24 K for $X=59.6$ and 0.06 K for $X=90.5$ mixture.
[14] K. Ema, G. Nounesis, C.W. Garland, and R. Shashidhar, Phys. Rev. A **39**, 2599 (1989).
[15] P. Sullivan and G. Seidel, Phys. Rev. **173**, 679 (1968).
[16] $\tau_e=RC_t$, where C_t is the sample heat capacity including the cell, and R is the thermal resistance between the sample and the heat bath. $\tau_i=L^2/\sqrt{90}D_T$, where L is the sample thickness and D_T is its thermal diffusivity and therefore $D_T\propto 1/C_t$. See Ref. [15].
[17] In a geometry where the heater and the thermometer are attached on opposite sides of a platelet sample, $a=1$ is obtained as described in Ref. [15]. If the heater and the thermometer are attached on the same side, we obtain $a=-\sqrt{10}$. Our measuring condition is close to the latter case.
[18] C. Bagnuls and C. Bervillier, Phys. Rev. B **32**, 7209 (1985); C. Bagnuls, C. Bervillier, D.I. Meiron, and B.G. Nickel, *ibid.* **35**, 3585 (1987).
[19] C.W. Garland, G. Nounesis, M.J. Young, and R.J. Birgeneau, Phys. Rev. E **47**, 1918 (1993).
[20] $D_1^+=D_1^-$ is expected from an ϵ-expansion calculation to first order in ϵ. See A. Aharony and G. Ahlers, Phys. Rev. Lett. **44**, 782 (1980).
[21] The values of D_1^+/D_1^- obtained from an ϵ-expansion to higher order and from field theory are only slightly larger than unity for the 3D XY universality class: 1.17 and 1.6, respectively. See V. Privman, P.C. Hohenberg, and A. Aharony, in *Phase Transitions and Critical Phenomena*, edited by C. Domb and J.L. Lebowitz (Academic, New York, 1991), Vol. 14.
[22] G. Nounesis, C.W. Garland, and R. Shashidhar, Phys. Rev. A **43**, 1849 (1991).
[23] A phase diagram which is closer to ours has been obtained recently from a dielectric measurement. See Fig. 5 in H. Uehara, Y. Iino, and J. Hatano, Jpn. J. Appl. Phys., Part 1 **36**, 6118 (1997).
[24] T.S. Chang, A. Hankey, and H.E. Stanley, Phys. Rev. B **8**, 346 (1973).
[25] The present case corresponds to Fig. 8 of Ref. [24], where h is interpreted as the field conjugate to the Sm-C* ordering, and h_2 is the concentration X.
[26] J.F. Nagle, Phys. Rev. A **2**, 2124 (1970); J.F. Nagle and J.C. Bonner, J. Chem. Phys. **54**, 729 (1971); J.C. Bonner and J.F. Nagle, J. Appl. Phys. **42**, 1280 (1971).
[27] Y. Takeuchi and I. Tatsuzaki, J. Phys. Soc. Jpn. **51**, 545 (1982), and references therein.
[28] H.Y. Liu, C.C. Huang, Ch. Bahr, and G. Heppke, Phys. Rev. Lett. **61**, 345 (1988).
[29] L. Benguigui and P. Martinoty, Phys. Rev. Lett. **63**, 774 (1989); J. Phys. II **7**, 225 (1997).